Work fluctuations in periodically driven chaotic systems

A Thesis

submitted to
Indian Institute of Science Education and Research Pune
in partial fulfillment of the requirements for the
BS-MS Dual Degree Programme

by

P Sravya

Indian Institute of Science Education and Research Pune
Dr. Homi Bhabha Road,
Pashan, Pune 411008, INDIA.

May, 2019

Supervisor: Dr. Bijay Kumar Agarwalla

Certificate

This is to certify that this dissertation entitle **Work fluctuations in periodically driven chaotic systems** towards the partial fulfilment of the BS-MS dual degree programme at the Indian Institute of Science Education and Research, Pune represents study/work carried out by P Sravya at Indian Institute of Science Education and Research under my supervision, during the academic year 2018-2019.

Dr. Bijay Kumar Agarwalla

Assistant Professor

Department of Physics

IISER Pune

Committee:

Dr. Bijay Kumar Agarwalla

Dr. Sreejith GJ

This thesis is dedicated to my dear parents.

Declaration

I hereby declare that the matter embodied in the report entitled **Work fluctuations in periodically driven chaotic systems** are the results of the work carried out by me at the Department of Physics, Indian Institute of Science Education and Research, Pune, under the supervision of **Dr. Bijay Kumar Agarwalla** and the same has not been submitted elsewhere for any other degree.

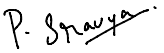

P Sravya

Acknowledgments

I am grateful to my supervisor Dr.Bijay Kumar Agarwalla for giving me this opportunity and for his constant support and guidance throughout this year. His interest towards his field of work has inspired me so much. I also want to thank my co-supervisor Dr. MS Santhanam for his time and all the valuable discussions we have had with him. I also take this opportunity to thank all my friends for making life happy when things were stressful. I want to thank Sandeep, Sruthy, Aanjaneya and Sushant for discussions that helped me understand many concepts better. Lastly, I want to thank my parents and my dear sister for bearing with me as well as being a constant support which has made me reach this point of my life.

Abstract

Fluctuation relations have been one of the recent discoveries that has helped us take a step in understanding how thermodynamics can be applied to small systems in the quantum regime. In this study we investigate the work distributions of a particular type of periodically driven chaotic system namely the kicked rotor system and the signatures of the system dynamics that are captured in these work distributions. We then verify the Crooks relation for this system. Finally, we examine the quantum-classical correspondence through numerical simulations at the level of work distributions and its moments for the chosen system which exhibits drastically different classical and quantum behaviour.

Contents

List of Figures

Chapter 1

Introduction

Any system at the microscopic level is made of matter that is in constant motion. Due to this the physical quantities associated with the system undergo fluctuations. These are thermal fluctuations which arise due to the temperature of the system. For quantum systems, quantum fluctuations also occur due to inherent quantum uncertainty of physical quantities. These fluctuations (relative) grow as $\frac{1}{\sqrt{N}}$ with the system size N. For large systems (in the thermodynamic limit), the mean of various physical quantities give a good enough description of the system. But as the system size decreases, these fluctuations become more and more significant. Therefore, it becomes prudent to study the distribution of the physical quantities of interest.

The Maxwell distribution of velocities for a gaseous system at equilibrium is a good example. For systems at equilibrium or weakly driven near equilibrium, the response of the system to any external perturbation is related to its small fluctuations. This is given by the universal fluctuation-dissipation theorem. Similar relations for systems driven far from equilibrium were not known until the end of last century when the exact fluctuation relations for classical systems far away from equilibrium were discovered [1],[2],[3],[5]. These focus on distributions of fluctuating quantities such as heat or work that characterize non-equilibrium transformations. Fluctuation relations put restrictions on the form of the probability density functions of these non-equilibrium fluctuating quantities and also explains the macroscopic irreversibility that is seen often in nature. They generally take the form

$$P_F(x) = P_R(-x)\ \exp[a(x-b)] \tag{1.1}$$

where $P_F(x)$ is the probability density function of the quantity x during the forward driving process and $P_B(x)$ is that of the reverse driving process. The constants a and b are dependent on the initial and final states of the system [5]. A good example is the work fluctuation relation which we will look at in the next chapter.The definitions of forward and reverse driving processes will be clarified in the next chapter.

These relations hold under conditions which are as follows.

1. The initial equilibrium state is described by the Gibbs canonical distribution,

$$\rho = \frac{e^{-\beta H}}{Z}$$

   where $Z = \mathrm{Tr} e^{-\beta H}$ is the partition function, with $\beta = \frac{1}{k_B T}$ being the inverse temperature.

2. The underlying microscopic dynamics of the system should be time-reversal invariant.

The exponential term that is in equation(1.1) emerges due to the $e^{-\beta H}$ term in the initial canonical distribution. Also, since there is a distribution of initial states, we get a distribution of work values each corresponding to the driving process starting from each initial state. The fluctuation relations hold true for an isolated system, a closed system (which can exchange energy with the bath when driving is happening) and an open system (can exchange both energy and particles). They also hold true for any system size.

In this work, we will be studying the work fluctuation relations. The chosen system of study is a chaotic system - the kicked rotor. A chaotic system shows varied and rich dynamics in different parameter regimes. We want to study the signature of these dynamics in work distributions in these different parameter regimes and also verify the work fluctuation relations. These work distributions depend on the type of driving. In the kicked rotor system the driving is periodic which simplifies both the analytical and the numerical aspects of the project. Another main focus would be on verification of the classical-quantum correspondence at the level of work distributions as the considered system shows very different classical and quantum behaviours for different kick strengths.

The outline for this thesis is as follows. In chapter 2, I will explain in detail about the work fluctuation relations in the classical and quantum case. In chapter 3, I will introduce the kicked rotor system and also talk about the floquet theory that will be used to study the quantum kicked rotor system. Chapter 4 consists of work distribution expressions for the quantum kicked rotor and in the final chapter 5, I will present the results and discussion.

Chapter 2

Work fluctuation theorem and Jarzynski equality

In this work we will particularly be studying the work fluctuation relations. Even long after the discovery of classical work fluctuation relations, there are some ambiguities regarding the definition of quantum work. I will present the current understanding of the classical and quantum work and also explain how the work fluctuation relation can be obtained from these definitions.
Consider a system in an initial equilibrium state A with the Hamiltonian H_A. Some driving is done to take the system out of equilibrium to some other state B with Hamiltonian H_B. This is referred to as the forward process. Let the system be an isolated driven system which does not remain in contact with the bath during the driving. The reverse process comprises of driving the system in the reverse manner starting from the equilibrium state at the same β described by the Hamiltonian H_B.

Similar to the general expression of fluctuation relations (1.1), the work fluctuation relation can be written as

$$P_F(W) = P_R(-W)\ e^{\beta(W-\Delta F)} \tag{2.1}$$

This is known as the Crooks relation [5].The β corresponds to the temperature of the initial states in both the forward and the reverse processes. The $W - \Delta F$ term is called the

dissipated work (entropy production) which would be zero for a reversible process. This equation can be simplified by integrating over all W values.

$$\int P_F(W)e^{-\beta W}dW = \int P_R(-W)e^{-\beta\Delta F}dW = e^{-\beta\Delta F}$$

Therefore,

$$\langle e^{-\beta W}\rangle = e^{-\beta\Delta F} \tag{2.2}$$

where the average is over the probability distribution of work. This equation is known as the Jarzynski equality(JE) [3],[4]. This equation implies that though we drive the system in an irreversible manner to a non-equilibrium final state starting from an equilibrium initial state, we can get the equilibrium free energy difference by driving it multiple times and then take an average. On applying the Jensen inequality i.e $\langle e^x\rangle \geq e^{\langle x\rangle}$ to JE, we get $\langle W\rangle \geq \Delta F$ which is an implication of the second law of thermodynamics. Therefore, the JE is often referred to as the microscopic representation of the second law. This implies that for any system under consideration, the average value of work done $\langle W\rangle$ is greater than the change in equilibrium free energy but the value of work in any single realisation can be lesser than ΔF. The possibility of this happening is more for smaller systems due to increased fluctuations.

Now we will discuss about the work fluctuation relations in classical and quantum descriptions.

2.1 Classical work fluctuation relation

Consider a classical system characterized by a Hamiltonian with $H_0(z)$ as the unperturbed part and the perturbation $-\lambda Q(z)$ due to the external force λ_t that couples to the coordinate $Q(z)$. Therefore, the Hamiltonian will be

$$H(z,\lambda_t) = H_0(z) - \lambda_t Q(z) \tag{2.3}$$

where $z = (q, p)$ corresponds to a point in phase space. The initial state is taken from the probability density, $\rho_0 = \frac{e^{-\beta H_0(z)}}{Z_0}$. We can understand the principle of microreversibility in the following way. For every initial point in the phase space $z_0 = (q_0, p_0)$, the system evolves to a point z_t at any time $t \in [0, \tau]$ which is determined by the force protocol. We can write

$$z_t = \psi_{t,0}[z_0; \lambda] \tag{2.4}$$

at time t, as a trajectory $\psi_{t,0}[z_0; \lambda]$ in the phase space which is a function of the initial point z_0 and a functional of the force protocol λ [6]. This trajectory represents the forward protocol. Now, provided the Hamiltonian H_0 is time reversal invariant, we can define the backward protocol $\tilde{\lambda}$ as

$$\tilde{\lambda}_t = \lambda_{\tau - t} \tag{2.5}$$

and the backward trajectory can be related to the forward trajectory as follows,

$$z_t = \psi_{t,0}[z_0; \lambda] = \epsilon \psi_{\tau - t, 0}[\epsilon z_\tau; \tilde{\lambda}] \tag{2.6}$$

where $\epsilon z = \epsilon(q, p) = (q, -p)$. This is expressed in a schematic in the figure (2.1).

Now after understanding of the system and the driving, we can think about the form of work to obtain the Crook's relation or the Jarzynski equality. We know from thermodynamics that,

$$\Delta E = W + Q$$

For an isolated driven system, Q is zero and hence we can write W as the change in energies of the final and the initial states. Therefore, we can define work [3] as

$$W[z_0; \lambda] = H(z_\tau, \lambda_\tau) - H(z_0, \lambda_0) \tag{2.7}$$

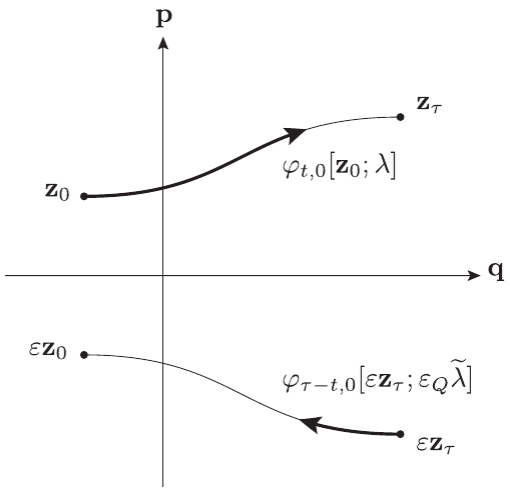

Figure 2.1: Microscopic reversibility in a classical Hamiltonian system. The state z_0 in the forward process evolves from $t = 0$ to t to the state $z_t = \psi_t(z_0, \lambda_t)$ upto $t = \tau$. In the reverse process, the initial state ϵz_τ evolves from $t = 0$ to $t = \tau - t$ to the state $\epsilon z_{\tau-t} = \psi_{\tau-t}(\epsilon z_\tau, \tilde{\lambda}_t)$ upto $t = \tau$ [6].

In terms of the force protocol, we can write work [4] as

$$W[z_0, \lambda] = \int_0^\tau dt\ \dot{\lambda}\ \frac{\partial H(z_t, \lambda_t)}{\partial \lambda_t} \tag{2.8}$$

Now consider,

$$\begin{aligned}\langle e^{-\beta W}\rangle &= \int dz_0\ \rho_0\ e^{-\beta W} \\ &= \frac{1}{Z_{\lambda_0}} \int dz_\tau \left|\frac{\partial z_0}{\partial z_\tau}\right|\ e^{-\beta(H(z_0,\lambda_0)+W)} \\ &= \frac{Z_{\lambda_\tau}}{Z_{\lambda_0}}\end{aligned}$$

Due to Liouville's theorem, $\left|\frac{\partial z_0}{\partial z_\tau}\right| = 1$. The free energy$(F)$ of an equilibrium state in terms of the partition function(Z) is $F = -k_B T \ln(Z)$. Therefore we get the Jarzynski equality,

$$\langle e^{-\beta W}\rangle = e^{-\beta(F_\tau - F_0)} = e^{-\beta \Delta F}$$

where $\beta = \frac{1}{k_B T}$.

For the case of closed system, the driving force is applied only to the system and hence the bath Hamiltonian and the interaction Hamiltonian remains unchanged and the definition of work given by the equation(2.7) still holds and Jarzynski equality can be derived in the same manner. Therefore, this proof can be extended to the closed and open systems as well [8],[9].

2.2 Quantum work fluctuation relation

The previous section dealt with the work fluctuations for a classical system. In this section we will look at work fluctuations for the quantum case. Now, the Hamiltonian $H(z, \lambda_t)$ will be replaced by operator $H(\lambda_t)$ and the probability density by the density matrix $\rho(\lambda_t)$,

$$\rho(\lambda_t) = \frac{e^{-\beta H(\lambda_t)}}{Z(\lambda_t)}$$

where $Z(\lambda_t) = \text{Tr } e^{-\beta H(\lambda_t)}$.

The principle of microreversibility can be understood in terms of the unitary operator which describes the driving process. If $U_t[\lambda]$ describes the forward process, then the reverse process can be described by $U_{\tau-t}[\tilde{\lambda}]$ [6]. These are related as,

$$U_{t,\tau}[\lambda] = \theta^\dagger \; U_{\tau-t,0}[\tilde{\lambda}] \; \theta \tag{2.9}$$

where θ is the quantum- mechanical time-reversal operator. So if $U_{\tau,0}[\lambda]$ takes an initial state $|i\rangle$ to a final state $|f\rangle$ in time t = 0 to τ then the reverse driving $U_{\tau-t,0}[\tilde{\lambda}]$ takes the time-reversed initial state $\theta|f\rangle$ to the final state $\theta|i\rangle$. It is important to note that to achieve time reversal, we need to change the sign of the momenta (this corresponds to applying θ) as well as reverse the sequence of Hamiltonians in time(it is a nonautonomous system).

Now we can look at the definition of quantum work which is challenging for the following reasons:

- The definition of work similar to equation(2.8) is not possible because the notion of trajectories breaks down in the case of quantum mechanics because of the inherent uncertainty in the position or momentum at each time step.
- The definition of work operator as $W = H(\lambda_t) - H(\lambda_0)$ is not possible as one cannot operate this on a single state to get a value of work. The two observables cannot be simultaneously observed as the Hamiltonians at different times don't commute.
- Also, we know from thermodynamics that work is not a state variable. Therefore, we cannot get the value by doing a single measurement on a single state.

Due to the above reasons, a method called two-time measurement is used to define quantum work. In the next section we discuss the two-time measurement and how to derive the fluctuation relations from the defined work for a quantum system.

2.2.1 Two-time measurement

In the two-time measurement method, the systems initial energy is measured at time $t = 0$, then the system is evolved through a unitary transformation upto some time t and the final energy of the system is again measured. Work is defined as the difference of the eigenvalues obtained in the initial and the final measurements.

$$W = E_f - E_i$$

where E_i and E_f are eigenvalues of initial and final Hamiltonians.

Now the work probability distribution can be defined as,

$$P(W) = \sum_{i,f} \delta(W - (E_f - E_i))\ P(E_f, E_i) \tag{2.10}$$

where $P(E_f, E_i)$ is the joint probability to measure E_i at time 0 and E_f at time t which can be expanded as follows,

$$P(E_f, E_i) = Tr\ [\hat{P}_{E_f}\ \hat{U}(t,0)\ \hat{P}_{E_0}\ \hat{\rho}_0\ \hat{P}_{E_0}\ \hat{U}^\dagger(t,0)\ \hat{P}_{E_f}] \tag{2.11}$$

where $\hat{P}_{a_i} = |a_i\rangle\langle a_i|$ is the projection operator. $\hat{P}_{E_0}\ \hat{\rho}_0\ \hat{P}_{E_0}$ corresponds to the density matrix after the measurement is done at $t = 0$. The term $\hat{U}(t,0)\ \hat{P}_{E_0}\ \hat{\rho}_0\ \hat{P}_{E_0}\ \hat{U}^\dagger(t,0)$ refers to the unitary evolution of the density matrix after the first measurement. And the projection operators at the ends represent the final measurement done on the evolved density matrix at time t. Now we consider two Hilbert space basis sets $|i, E_i\rangle$ and $|j, E_f\rangle$ (corresponding to different times) where i and j represent degenerate eigenstates [7].

$$P(E_f, E_i) = \sum_{i,f} P[j, E_f; i, E_i] = \sum_{i,f} P(j, E_f/i, E_i)\ P(i, E_i) \tag{2.12}$$

where,

$$P(j, E_f/i, E_i) = |\langle j, E_f|\hat{U}(t,0)|i, E_i\rangle|^2 \tag{2.13}$$

$$P(i, E_i) = \langle i, E_i|\hat{\rho}_0|i, E_i\rangle \tag{2.14}$$

The probability distribution for W is given by the difference in the values E_f and E_i and is given by equation(2.10). In order to show the Jarzynski equality, it is convenient to work with the generating function associated with this distribution. The generating function can be written as

$$G(u) = \int_{-\infty}^{\infty} dW e^{-iuW}\ P(W) = \sum_{E_i,E_f} e^{-iu(E_f - E_i)}\ P(E_f, E_i) \tag{2.15}$$

The n^{th} derivative of generating function with respect to u evaluated at $u = 0$ gives the n^{th} moment i.e

$$\langle W^n\rangle = (-i)^n\ \frac{\partial^n}{\partial u^n} G(u)\bigg|_{u=0}$$

Now we put equation(2.11) into the equation(2.15) to simplify the expression for generating function.

$$G(u) = \sum_{E_i,E_f} e^{iu(E_f - E_i)}\ Tr\ [\hat{P}_{E_f}\ \hat{U}(t,0)\ \hat{P}_{E_0}\ \hat{\rho}_0\ \hat{P}_{E_0}\ \hat{U}^\dagger(t,0)\ \hat{P}_{E_f}] \tag{2.16}$$

$$G(u) = Tr\ [\hat{P}_{E_0}\ \hat{\rho}_0\ \hat{P}_{E_0} \sum_{E_i} e^{-iuE_i}\ \hat{P}_{E_0}\ \hat{U}^\dagger(t,0)\ \sum_{E_f} e^{iuE_f} \hat{P}_{E_f} \hat{U}(t,0)] \tag{2.17}$$

using the properties,

$$\hat{P}_{a_i}^2 = \hat{P}_{a_i}$$
$$\sum_{a_i} a_i \hat{P}_{a_i} = \tilde{A}$$

where $\tilde{A}$ is the operator whose eigenvalues are a_i, $G(\lambda)$ can further be simplified as follows.

$$G(u) = Tr\ [\bar{\hat{\rho}_0} e^{-iuH(0)}\ \hat{U}^\dagger(t,0)\ e^{iuH(t)}\hat{U}(t,0)] \tag{2.18}$$
$$\bar{\hat{\rho}_0} = \sum_{E_0} \hat{P}_{E_0}\ \hat{\rho}_0\ \hat{P}_{E_0}$$

Now, if the initial density matrix doesn't have any coherences i.e if $[H(0), \hat{\rho}_0] = 0$, then $[\hat{P}_{E_0}, \hat{\rho}_0] = 0$ as $H_0 = \sum_{E_0} E_0 \hat{P}_{E_0}$. This implies that the projection operator and the density matrix can be flipped inside the trace. Therefore,

$$\bar{\hat{\rho}_0} = \sum_{E_0} \hat{P}_{E_0}\ \hat{\rho}_0\ \hat{P}_{E_0} = \sum_{E_0} \hat{\rho}_0 \hat{P}_{E_0}^2 = \hat{\rho}_0 \tag{2.19}$$

Therefore, the simplified expression of the generating function that will help us obtain the Jarzynski equality is

$$G(u) = \left\langle e^{-iuH(0)}\ \hat{U}^\dagger(t,0)\ e^{iuH(t)}\hat{U}(t,0) \right\rangle_{\hat{\rho}_0} \tag{2.20}$$

If we choose the initial density matrix as $\rho_0 = \frac{e^{-\beta H(0)}}{Z_0}$ then we have,

$$G(u) = \frac{1}{Z_0} Tr\ [e^{-\beta H(0)} e^{-iuH(0)} e^{+iuH^H(t)}] \tag{2.21}$$

Now consider $\lambda = i\beta$ and $Z_t = Tr\ [e^{-\beta H(t)}]$ then

$$G(i\beta) = \frac{1}{Z_0} Tr[e^{-\beta H(t)}] = \frac{Z_t}{Z_0} \tag{2.22}$$

And as the partition function can be related to the free energy as $F = -(\ln Z)/\beta$, we get

$$\langle e^{-\beta W} \rangle = G(i\beta) = e^{-\beta \Delta F}$$

Therefore, we obtain the Jarzynski equality by using the definition of work given by the two-time measurement. Although the quantum Jarzynski equality can be proven analytically, there have been many challenges to experimentally verify this due to the limitations of the projective measurements done on a quantum system.

The Crooks relation can be proven in a similar manner. The following equation is a symmetry relation of the generating function which can be derived using the principle of microreversibility [6].

$$Z_0 \; G(u, \lambda) = Z_\tau \; G(-u + i\beta, \tilde{\lambda}) \tag{2.23}$$

where $G(u, \lambda)$ corresponds to the forward process and $G(-u + i\beta, \tilde{\lambda})$ correspond to the reverse process. Upon taking the inverse fourier transform on both sides, and using the properties of the fourier transform, if $f(\eta)$ is the fourier transform of $f(x)$ and if $h(x) = f(x - x_0)$ then the fourier transform of $h(x)$ is $e^{-ix_0\eta} \; f(\eta)$, we get

$$Z_0 \; P(W, \lambda) = Z_\tau \; e^{\beta W} \; P(-W, \tilde{\lambda}) \tag{2.24}$$

$$\frac{P(W, \lambda)}{P(-W, \tilde{\lambda})} = e^{\beta(W - \Delta F)} \tag{2.25}$$

This is the Crooks relation. The following chapters will talk about the system we chose for this study and also how we can understand the properties of work for this system.

Chapter 3

Kicked rotor and the Floquet theory

In this chapter I will introduce the system that we study in this work which is the kicked rotor. It is a periodically driven system which shows chaotic dynamics in different regimes determined by a driving parameter. Another interesting point to note is that chaotic behaviour of the classical kicked rotor system vanishes in its quantum analogue. Instead the system exhibits dynamical localization which can also be connected to the Anderson localization studied in the field of condensed matter physics [15]. Here I will only be talking about the kicked rotor system and dynamical localization.

3.1 Kicked rotor system

The kicked rotor system is characterized by the Hamiltonian,

$$H(t) = \frac{L^2}{2} + k\cos(\theta) \sum_n \delta(t-n) \tag{3.1}$$

and it describes the free rotation of a pendulum with angular momentum L and is periodically kicked by applying a potential whose strength is given by k. The moment of inertia I and the time period of the kicking τ is normalized to 1.

3.1.1 Classical description

This system can be studied classically by discretizing the time of evolution of the system and solving the Hamilton's equations in this discrete time intervals. Therefore, the equations of motion take the form of a discrete map which in this case is the Standard map [10] ,[11].

$$\theta_{n+1} = \theta_n + L_{n+1} \tag{3.2}$$

$$L_{n+1} = L_n + k \sin\theta_n \tag{3.3}$$

This simple system can show complex behaviour which is studied using the Kolmogorov-Arnold-Moser theory which represents the regular ballistic flow with tori. For small values of k, the system shows regular ballistic behaviour for any initial condition. There is a critical value of $k \approx 1.97$ where chaos starts to set in. As k is increased, the system becomes more and more chaotic and for $k > 5$ most of the regular parts disappear [12]. This can be shown in the phase space plots shown in the figure (3.1).Therefore, as k is increased the system becomes diffusive. When $|L_n|$ becomes greater that 2π, then the consecutive θ_n become uncorrelated and the sign of $\sin\theta$ becomes random. This implies that the evolution of L_n is like a random walk. A more quantitative description is given by the function $f_N(\Delta L)$ which is the probability that after N kicks, $L_n - L_0$ takes the value ΔL i.e

$$f_N(\Delta L) = \langle \delta(\Delta L - L_n + L_0) \rangle \tag{3.4}$$

where the averaging is over all the initial conditions. We can write the delta function in terms of its Fourier integral so as to evaluate the average in the above equation [10].

$$f_N(\Delta L) = \left\langle \frac{1}{2\pi} \int_{-\infty}^{\infty} dt\ e^{i(\Delta L - L_n + L_0)t} \right\rangle \tag{3.5}$$

$$= \left\langle \frac{1}{2\pi} \int_{-\infty}^{\infty} dt\ e^{i(\Delta L t}\ \Pi_{n=0}^{n-1}\ e^{-i(L_n - L_0)t} \right\rangle \tag{3.6}$$

$$= \left\langle \frac{1}{2\pi} \int_{-\infty}^{\infty} dt\ e^{i(\Delta L t}\ \Pi_{n=0}^{n-1}\ e^{-ikt\sin\theta_n} \right\rangle \tag{3.7}$$

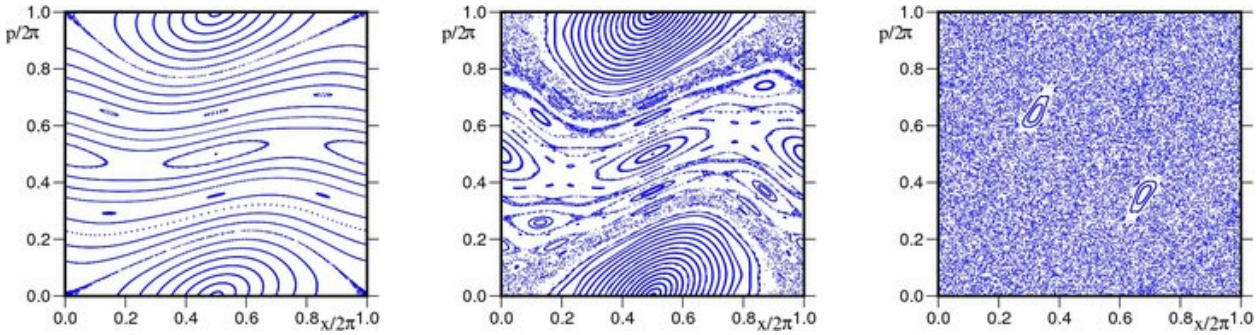

Figure 3.1: Phase space plots for the classical kicked rotor showing different behaviour for different kick strengths $k = 0.5$, 0.9716 and 5 respectively [13].

Now we take the k large limit where the successive θ_n become uncorrelated and therefore the averages on the right hand side can be calculated independently as,

$$\langle e^{-ikt\sin\theta}\rangle = \frac{1}{2\pi}\int_0^{2\pi} e^{-ikt\sin\theta}\, d\theta = J_0(kt) \tag{3.8}$$

where $J_0(kt)$ is the Bessel function. Putting this in the $f_N(\Delta L)$ equation, we get

$$f_N(\Delta L) = \frac{1}{2\pi}\int_{-\infty}^{\infty} dt\; e^{i\Delta Lt}\; [J_0(kt)]^N \tag{3.9}$$

For large N,

$$[J_0(kt)]^N = e^{N\ln J_0(kt)} = \exp\big(-\frac{N}{4}(kt)^2 + ...\big) \tag{3.10}$$

Therefore, in the $N \to \infty$ the equation (3.9) can be written as,

$$f_N(\Delta L) = \frac{1}{k\sqrt{\pi N}}\exp(-\frac{(\Delta L)^2}{k^2\; N}) \tag{3.11}$$

Then the average $\langle(\Delta L)^2\rangle$ is given by the following form and increases linearly with N.

$$\langle(\Delta L)^2\rangle = \frac{k^2}{2}N \tag{3.12}$$

The Gaussian form of $f_N(\Delta L)$ and the linear increase of the quadratic average indicates that this is a diffusive process with diffusion constant

$$D = \frac{k^2}{2\tau} \tag{3.13}$$

in our case $\tau = 1$.

This is only for the large k limit and when the diffusion constant is plotted as a function of time, we observe oscillations about the $k^2/2$ form which occurs due to the residual correlations between the successive kicks [14]. An improved expression for the diffusion constant is given by,

$$D = \frac{k^2}{4\tau}(1 - 2J_2(k) + 2J_2^2(k)) \tag{3.14}$$

where J_2 is an ordinary Bessel function. This was simulated and observed as shown in the figure (3.2). The points that are out of the improved expression trend are due to the remnant ballistic behaviour areas in the phase space which are referred to as the accelerator modes.

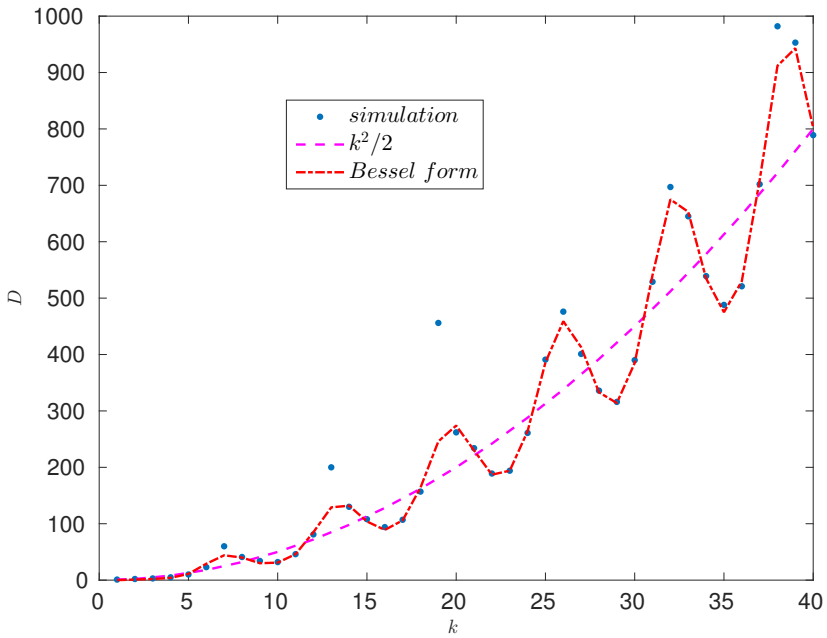

Figure 3.2: Diffusion constant as a function of kick strength k.

3.2 Floquet theory

We will look at the general idea of the Floquet theory that can be used to study the quantum kicked rotor system. Consider a Hamiltonian which had a periodic dependence on time given by,

$$H(t) = H_0 + V(t) \tag{3.15}$$

where $V(t+\tau) = V(t)$ and H_0 corresponds to the time independent part of the Hamiltonian. As the Hamiltonian has an explicit time dependence, we cannot solve the time-dependent Schrodinger equation using the ansartz,

$$\psi_n(x,t) = \exp\big(-\frac{i}{\hbar}E_n\ t\big)\ \psi_n(x) \tag{3.16}$$

We know that E is no longer time independent but H is still invariant for discrete time steps of τ interval each. Therefore, we can find solutions $\psi_n(x,t)$ of the time independent Schrodinger equation that is also the common eigenbasis of the time translation shift operator T_τ [10] i.e

$$T_\tau\ \psi_n(x,t) = \psi_n(x,t+\tau) = \lambda_n\ \psi_n(x,t) \tag{3.17}$$

For these wavefunctions to be stationary, λ_n must be a phase factor, therefore

$$\psi_n(x,t+\tau) = e^{-i\phi_n}\psi_n(x,t) \tag{3.18}$$

which implies that $\psi_n(x,t)$ can take the form

$$\psi_n(x,t) = e^{-i\omega_n t}u_n(x,t) \tag{3.19}$$

where $u_n(x,t+\tau) = u_n(x,t)$ and $e^{-\omega_n t} = e^{-i\phi_n}$. The $u_n(x,t)$ are called the floquet modes and ω_n are called the quasi-energies as they form the eigenvalues of an effective Hamiltonian referred to as the Floquet Hamiltonian. We can write the total wavefunction as,

$$|\psi(t)\rangle = \sum_n e^{-i\omega_n t}\ a_n\ |u_n(t)\rangle \tag{3.20}$$

where $a_n = \langle u_n(t)|\psi(0)\rangle$ which will give the above equation a form of evolved state due to the Floquet Hamiltonian. Substituting this form of a_n in the above equation, we get an

effective form of unitary time evolution operator as shown below.

$$|\psi(t)\rangle = \sum_n e^{-i\omega_n t}\langle u_n(t)|\psi(0)|u_n(t)\rangle \tag{3.21}$$

$$= \sum_n e^{-i\omega_n t}|u_n(t)\rangle\langle u_n(t)|\psi(0)\rangle \tag{3.22}$$

This implies the unitary time evolution operator can be written as

$$U(t,0) = \sum_n e^{-i\omega_n t}\ |u_n(t)\rangle\langle u_n(t)| \tag{3.23}$$

For $t = \tau$, we can write simplify the equation by using the periodic property of the floquet modes $u_n(t+\tau) = u_n(t)$ to

$$U(\tau,0) = \sum_n e^{-i\omega_n \tau}\ |u_n(0)\rangle\langle u_n(0)| \tag{3.24}$$

This is like an eigenvalue equation for the unitary time evolution operator with eigenvalues $e^{-i\omega_n\tau}$ and the floquet modes $u_n(0)$ being the eigenvectors. $U(\tau,0)$ is called the Floquet operator.

The unitary time evolution operator for various times can be written as $U(t+N\tau,0) = U(t,0)U(N\tau,0)$ and $U(N\tau,0) = [U(\tau,0)]^N$ []. Therefore, we can study the system stroboscopically, i.e, see how the system has changed after every time period just by knowing the Floquet operator for the system.

3.2.1 Floquet operator for a periodically kicked system

We will derive a general form of the floquet operator for a delta kicked system in this section. Lets begin with the Hamiltonian that describes such a system.

$$H(t) = H_0 + V_0 \sum_N \delta(t - N\tau) \tag{3.25}$$

To proceed lets replace for time being the delta function with a pulse having a finite width $\Delta\tau$ and height $(\Delta\tau)^{-1}$ [5]. And the Hamiltonian can be written as

$$H(t) = \begin{cases} H_0 & n\tau < t < (n+1)\tau - \Delta\tau \\ H_0 + \frac{1}{\Delta\tau}V_0 & (n+1)\tau - \Delta\tau < t < (n+1)\tau \end{cases}$$

The time evolution operator $U(t)$ can be obtained directly as the Hamiltonian is piecewise constant. For $0 < t < \tau - \Delta\tau$,

$$U(t) = \exp\left(-\frac{i}{\hbar}H_0 t\right) \tag{3.26}$$

and for $\tau - \Delta\tau < t < \tau$,

$$U(t) = \exp\Big[-\frac{i}{\hbar}(H_0 + \frac{1}{\Delta\tau}V_0)(t - \tau + \Delta\tau)\Big]\ U(\tau - \Delta\tau) \tag{3.27}$$

As the Floquet operator is $U(\tau)$, we get

$$F = \exp\Big[-\frac{i}{\hbar}(H_0 + \frac{1}{\Delta\tau}V_0)\Delta\tau\Big]\ \exp\Big(-\frac{i}{\hbar}H_0(\tau - \Delta\tau)\Big) \tag{3.28}$$

In the limit $\Delta\tau \to 0$, we can separate the first term into two exponentials and we get the following form.

$$F = \exp\Big(-\frac{i}{\hbar}V_0\Big)\exp\Big(-\frac{i}{\hbar}H_0\tau\Big) \tag{3.29}$$

In the next section this general form is used to get a form for the floquet operator of the quantum kicked rotor system.

3.2.2 Quantum kicked rotor system

The kicked rotor is described by the Hamiltonian,

$$H(t) = \frac{L^2}{2} + k\cos\theta\sum_n \delta(t - n) \tag{3.30}$$

where the moment of inertia I and the time period τ are taken to be 1.

From equation (3.29), the floquet operator for this system can be written as,

$$F = \exp(-\frac{i}{\hbar}k\cos\theta)\exp(-\frac{i}{\hbar}\frac{L^2}{2}\tau) \tag{3.31}$$

Floquet modes corresponding to this floquet operator can be written in terms of the eigenbasis of the operator $L^2 = -\hbar^2\frac{\partial^2}{\partial\theta^2}$. The eigenbasis of L^2 operator is given by,

$$\psi_n = \langle\theta|n\rangle = \frac{1}{\sqrt{2\pi}}\exp(in\theta)$$

Therefore, $F_{mn} = \langle m|F|n\rangle$ takes the form,

$$F_{mn} = \frac{1}{2\pi}\int_0^{2\pi}\exp(-im\theta)\ \exp(-\frac{i}{\hbar}k\cos\theta)\ \exp(-\frac{i}{\hbar}\frac{L^2}{2}\tau)\ \exp(in\theta)\ d\theta$$

$$F_{mn} = \exp(-\frac{i}{\hbar}\frac{n^2\hbar^2}{2}\tau)\ i^{n-m}\ J_{n-m}(\frac{k}{\hbar}) \tag{3.32}$$

where $J_{n-m}(\frac{k}{\hbar})$ is the bessel function. This expression will be used to construct the Floquet operator numerically.

The evolution of the system can be directly calculated using this form of the floquet operator starting from any given initial state. Lets assume $a(\theta)$ to be the probability of the rotor being at an initial angle θ, then the initial state in the angular momentum basis is given by,

$$A_0 = \begin{pmatrix} a_1 \\ a_2 \\ . \\ . \\ . \end{pmatrix}$$

where a_n is the fourier transform of the $a(\theta)$ i.e

$$a_n = \frac{1}{2\pi}\int_0^{2\pi} a(\theta)e^{-in\theta}\, d\theta \tag{3.33}$$

Now an evolved state can be written as,

$$A_N = F^N A_0 \tag{3.34}$$

We saw in the earlier section that the $\langle L^2\rangle$ for the classical system increases linearly with N. Here we get the quantum mechanical $\langle L^2\rangle$ so as to compare it with the classical one.

$$\langle L^2\rangle = A_N^\dagger\ L^2\ A_N \tag{3.35}$$

where we can use the expression of A_N in terms of A_0 to simplify. When $\langle L^2\rangle$ is plotted as a function of number of kicks, we get a trend that is very different from the classical one. The region where the classical system shows chaotic behaviour, the quantum system exhibits localization as shown in the figure (3.3). To understand this, we first consider the expression of $\langle L^2\rangle$ in terms of the floquet modes and eigenvalues [10] i.e

$$\langle L^2\rangle = \sum_{i,j,q} e^{+(\omega_j-\omega_i)N\tau}\ \frac{\hbar^2 q^2}{2\pi}\ \langle n|u_i\rangle\ \langle u_i|q\rangle\ \langle q|u_j\rangle\ \langle u_j|n\rangle \tag{3.36}$$

This is obtained for ground state initial condition i.e starting with $l = 0$ state. From the expression, it is evident that the N dependence is in the exponential term which keeps oscillating. When $\ln(f_N(L))$ is plotted, a distribution occurs which suggests an exponential localization,

$$f_N(L) = \frac{1}{l_s}\exp\left(-\frac{2|L|}{l_s}\right) \tag{3.37}$$

where l_s is known as the localization length. For kick number $N < l_s$, the system fails to recognise the discrete spectrum and hence exhibits classical diffusive behaviour. But for the case $N > l_s$, the exponential term in the $\langle L^2\rangle$ expression oscillates very rapidly and

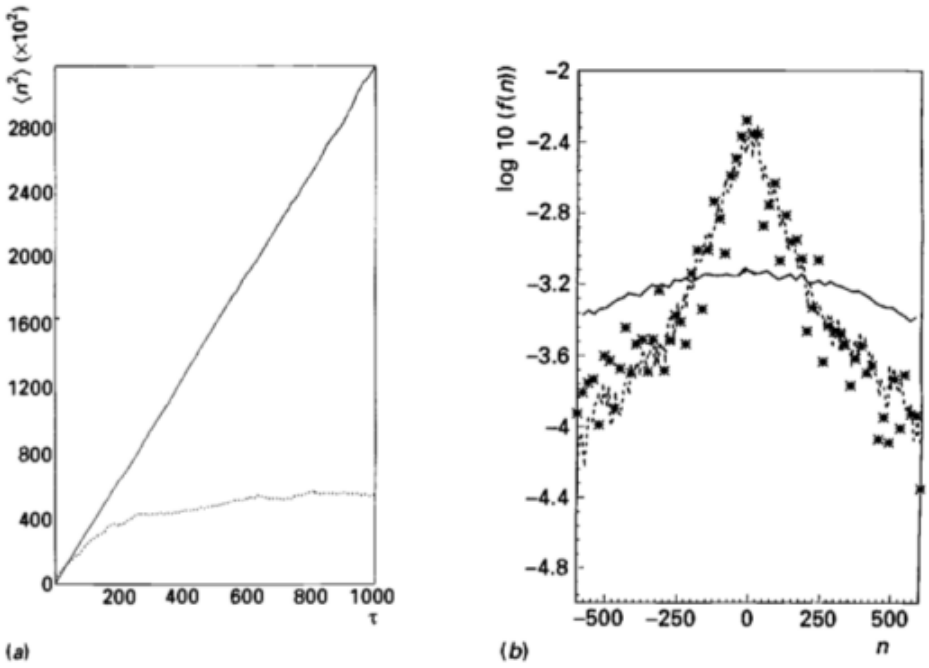

Figure 3.3: Dynamical localization in a quantum kicked rotor for $k = 5$ [10].

therefore cancels out to give an expression that is independent of N. We look for signatures of dynamical localization in the work distribution and its moments. These will be discussed in the chapter (5), on numerical results and discussion.

Chapter 4

Work distributions for the quantum kicked rotor

In the last chapter, we looked at the classical and quantum versions of kicked rotor and how different the behaviour is after large number of kicks for large kick strengths. We also got an idea of the floquet theory which will help us study the quantum version of the kicked rotor. In this chapter, we will get the quantum work distribution forms with the help of the floquet theory.

Using the two-time measurement method, we can write work to be $W = E_f - E_i$ and the work distribution can be written as,

$$P(W) = \sum_{i,f} \delta(W - (E_f - E_i)) \left|\langle f|U(t,0)|i\rangle\right|^2 P(i) \tag{4.1}$$

where $U(t,0)$ is the unitary time evolution operator that captures the driving. In the case of kicked rotor $U(\tau,0) = F$.

For the single kick case, we can write

$$P_F(W,\tau) = \sum_{m,n} \delta(W - (E_m - E_n)) \left|\langle m|U(\tau,0)|n\rangle\right|^2 P^0(n) \tag{4.2}$$

$$= \sum_{m,n} \delta(W - (E_m - E_n)) \left|\langle m|F|n\rangle\right|^2 P^0(n) \tag{4.3}$$

$$= \sum_{m,n} \delta(W - (E_m - E_n)) \langle m|F|n\rangle \langle n|F^\dagger|m\rangle P^0(n) \tag{4.4}$$

where m, n corresponds to the angular momentum basis states. Both $\langle m|F|n\rangle = F_{mn}$ and $\langle n|F^\dagger|m\rangle = F^\dagger_{nm}$ can be calculated as shown in the previous section.

$$\begin{aligned} F_{mn} &= \langle m| \exp(-\frac{k}{\hbar}\cos(\theta)) \ \exp(-i\frac{L^2}{2}\tau)|n\rangle \\ &= \exp(-\frac{i}{\hbar}\frac{n^2\hbar^2}{2}\tau) \ i^{n-m} \ J_{n-m}(\frac{k}{\hbar}) \end{aligned} \tag{4.5}$$

Similarly,

$$\begin{aligned} F^\dagger_{nm} &= \langle n| \exp(+i\frac{L^2}{2}\tau) \ \exp(+\frac{k}{\hbar}\cos(\theta))|m\rangle \\ &= \exp(+\frac{i}{\hbar}\frac{n^2\hbar^2}{2}\tau) \ i^{m-n} \ J_{m-n}(-\frac{k}{\hbar}) \end{aligned} \tag{4.6}$$

Therefore,

$$F^\dagger_{nm} = (F_{mn})^* \tag{4.7}$$

Hence we can write the work distribution for single kick as,

$$P_F(W,\tau) = \sum_{m,n} \delta(W - (E_m - E_n)) \left|F_{mn}\right|^2 P^0(n) \tag{4.8}$$

The $\left|F_{mn}\right|^2$ term is equal to $J^2_{n-m}(\frac{k}{\hbar})$ and therefore $P_F(W,\tau)$ can be simplified to

$$P_F(W,\tau) = \sum_n \delta(W) \ J_0^2(\frac{k}{\hbar}) \ P^0(n) + \sum_{m,n} \delta(W - (E_m - E_n)) \ J^2_{n-m}(\frac{k}{\hbar}) \ P^0(n) \tag{4.9}$$

$$P_F(W,\tau) = \delta(W)\ J_0^2(\frac{k}{\hbar}) + \sum_{m,n} \delta(W - (E_m - E_n))\ J_{n-m}^2(\frac{k}{\hbar})\ P^0(n) \tag{4.10}$$

The floquet operator elements are created using the equation (4.5), and the equation(4.8) is used to obtain the work distributions. From equation (4.10) it is clear that the probability of any work value is given by a bessel function of order equal to the difference in the momentum levels. As the value of bessel function decreases as the order increases, the probability of remaining in the same state is more probable when only 1 kick is applied to the system. This is also observed in the numerical simulation of work distribution shown in the figure (4.1 and 4.2). From figure (4.2) it can also be inferred that the work distribution seems to follow the Crooks relation i.e the probability of occurrence of a negative work value is less than that of the corresponding positive work and this decreases as the value of work is increased. To quantify this, we tried to plot $\ln[\frac{P_F(W)}{P_B(-W)}]$ versus W and check for the slope which is expected to be $1/T$ value considered in the simulation.

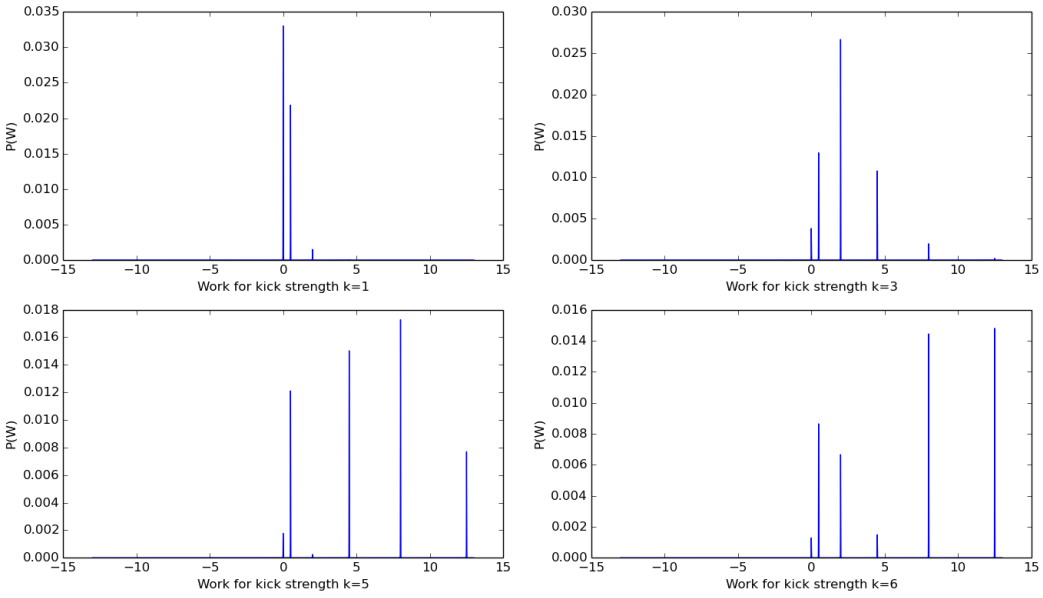

Figure 4.1: Work distributions after 1 kick, with ground state initial conditions i.e $T = 0$ for k values 1,3,5 and 6.

Now lets move to the case of N kicks. Similar to equation (4.1) we can write for the form

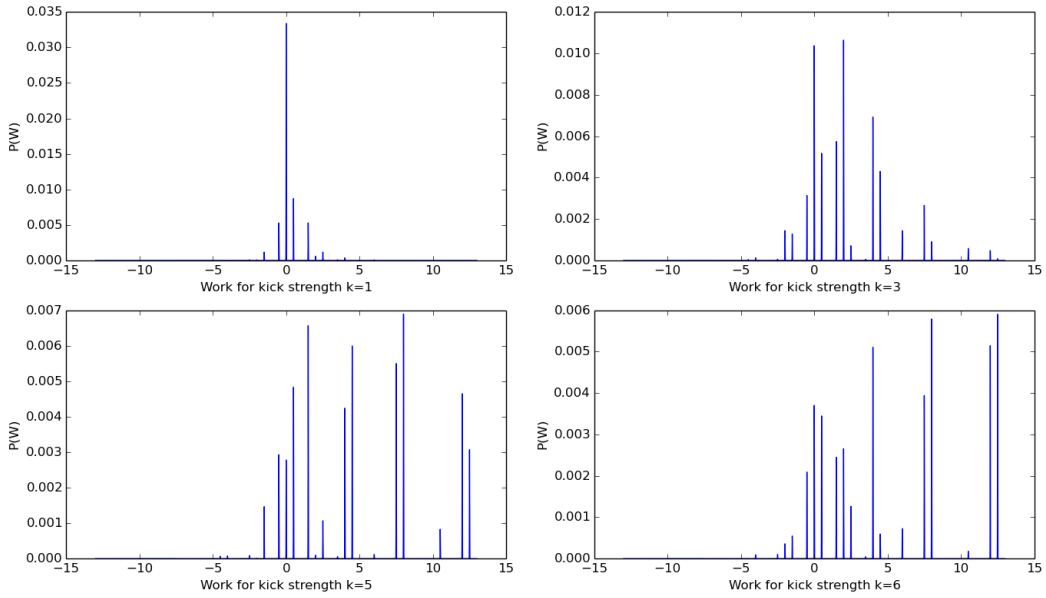

Figure 4.2: Work distributions after 1 kick, with canonical initial state with $T = 1$ for k values 1,3,5 and 6.

of work distribution after N kicks as,

$$P_F(W, N\tau) = \sum_{m,n} \delta(W - (E_m - E_n)) \left|\langle m|U(\tau, 0)^N|n\rangle\right|^2 P^0(n) \tag{4.11}$$

$$P_F(W, N\tau) = \sum_{m,n} \delta(W - (E_m - E_n)) \left|\langle m|F^N|n\rangle\right|^2 P^0(n) \tag{4.12}$$

We can express the floquet operator in terms of the floquet modes and its eigenvalues.

$$F = \sum_i \exp(-i\epsilon_i\tau)|\phi(0)\rangle\langle\phi(0)| \tag{4.13}$$

Using the orthonormality property of the floquet modes, we get

$$F^N = \sum_i \exp(-i\epsilon_i N\tau)|\phi(0)\rangle\langle\phi(0)| \tag{4.14}$$

Putting this in the work distribution,

$$P_F(W, N\tau) = \sum_{n,m} \delta(W - (E_m - E_n))\ \langle m|F^N|n\rangle\ \langle n|(F^\dagger)^N|m\rangle P^0(n) \tag{4.15}$$

$$P_F(W, N\tau) = \sum_{n,m,i,j} \delta(W - (E_m - E_n))\ \langle m|\exp(-i\epsilon_i N\tau)|\phi(0)\rangle\langle\phi(0)||n\rangle$$
$$\langle n|\ \exp(+i\epsilon_i N\tau)\ |\phi(0)\rangle\langle\phi(0)|m\rangle\ P^0(n) \tag{4.16}$$

Therefore, the work distribution for N kick case can be written as follows,

$$P_F(W, N\tau) = \sum_{n,m,i,j} \delta(W - (E_m - E_n))\ \exp(-i(\epsilon_i - \epsilon_j)N\tau)\ \langle m|\phi_i(0)\rangle\ \langle\phi_i(0)|n\rangle$$
$$\langle n|\phi_j(0)\rangle\ \langle\phi_j(0)|m\rangle\ P^0(n) \tag{4.17}$$

In the asymptotic limit, i.e when $N \to \infty$, only the $\epsilon_i = \epsilon_j$ terms will contribute and hence we get the following simplified form.

$$P_F(W, N\tau) = \sum_{n,m,i} \delta(W - (E_m - E_n))\ |\langle m|\phi_i(0)\rangle|^2\ |\langle\phi_i(0)|n\rangle|^2\ P^0(n) \tag{4.18}$$

We cannot simplify equation (4.17) further without having the knowledge about the floquet modes. Hence we will have to use numerical simulations to obtain work distribution. Once we get the floquet modes and the eigenvalues in terms of the angular momentum basis, we can use the equation (4.17) to obtain the work distributions numerically. Before trying to plot the work distributions for large number of kicks, we were interested in looking at the trends of the average and the variance of these work distributions as a function of number of kicks. In the next chapter, I will show the numerical simulations done to examine these trends. And then I will also discuss about the simulated work distributions for the N kick case.

Chapter 5

Numerical results and discussion

The analytical expression for work distributions for $N > 1$ kicks is limited to equation(4.17) as mentioned in the previous chapter. Therefore, we have to resort to numerical methods to obtain the work distributions after large number of kicks. Numerical simulation for large number of kicks comes with complications. As we approximate the number of momentum states available for the system, this has to be large enough when large number of kicks are given to the system or when the temperature is high. To handle large system sizes we need more computational power and time. Hence to get an idea of the work distributions before actually simulating them, we looked at the trends of the average and the variance of these work distributions and verified if they match with the expected trends. We also looked at the Quantum-Classical correspondence at the level of average and variance of work about which I will discuss. Finally, I will talk about the work distributions after N kicks.

5.1 Some important numerical details

5.1.1 Classical simulation

For simulating the classical system, we start with some initial θ and L value from a random uniform distrbution. We then evolve these values using the standard map. This is done multiple times (100,000 realisations were used in our study) so as to get the required average

values. For the case of work distributions we plot a histogram with all the work values from different realisations. For $T = 0$ case, we take the initial $L = 0$ for all the realisations. For $T \neq 0$, so as to incorporate the temperature into the initial state, we take L values from the distrbution,

$$\rho(L) = \frac{1}{\sqrt{2\pi\langle L^2\rangle}} \exp\big(-\frac{L^2}{2\langle L^2\rangle}\big)$$

which is nothing but a normal distrubtion with mean zero and variance equal to $\sqrt{k_B T}$ (k_B is the Boltzmann constant).This is using the fact that $\frac{\langle L^2\rangle}{2} = \frac{k_B T}{2}$ following from the equipartition theorem.

5.1.2 Quantum simulation and Hilbert space truncation

For the quantum case, we primarily work in the angular momentum basis. System is decsribed by the angular momentum eigenstates and the floquet operator which is used to evolve the system is also written in the angular momentum basis.We consider some '$2m+1$' (-m to $+m$) angular momentum states to represent the system. For any particular value of k or N, the converge of the required trends is used to decide where to truncate. However, this varies for different cases. When the temperature of the system is increased, it is expected that the number of states accessed will increase. Also, when trying to verify the quantum-classical correspondence i.e when we take the limit $\hbar \to 0$, the number of states of the system should increase. This can crudely be understood as follows. We know that the eigenvalues of the L operator are of the form $\hbar m$. Therefore, to attain a particluar L value the system has to attain a larger m value as $\hbar$ becomes smaller. Also, one would expect that as $\hbar \to 0$ the system would go from a discrete energy system to a more continuous system.

For $T = 0$, the initial state of the system is considered to be the zero momentum state. For $T \neq 0$, the initial state is taken from the canonical distribution given by the density operator,

$$\begin{aligned}\rho_0 &= \frac{e^{-\beta H_0}}{Z} \\ &= \sum_m \frac{e^{-\beta\frac{(\hbar m)^2}{2}}}{\sum e^{-\beta\frac{(\hbar m)^2}{2}}} \; |m\rangle\langle m|\end{aligned}$$

The average work values are calculated from the trace $\mathrm{Tr}[(H_N - H_0)\rho_0]$ where H_N is the

hamiltonian after N kicks and H_0 is the initial hamiltonian.The work distribution is given by the form,

$$P(W) = \sum_{m,n} \delta(W - (E_m - E_n)) \left|\langle m|F^N|n\rangle\right|^2 P^0(n)$$

where the transition probability term $\left|\langle m|F^N|n\rangle\right|^2$ is the product of F_{mn} and its complex comjugate. In order to numerically deal with the delta function, we use a gaussian representation of the dirac delta function which is given by,

$$\delta(W - (E_m - E_n)) = \lim_{\eta \to 0} \frac{1}{\eta\sqrt{\pi}} \exp[-\Big(\frac{(W - (E_m - E_n))}{\eta}\Big)^2]$$

where η is a parameter which is taken to be some small value in the numerics.

5.2 Average and Variance of Work

The work obtained from two-time measurement is defined as $W = E_f - E_i$ and this value for the case of the kicked rotor is given by,

$$W = E_f - E_i = \frac{L^2}{2} - \frac{L_{in}^2}{2}$$

We can see that work is directly proportional to the change in the square of angular momentum. Therefore we expect dynamical localization in the average work as a function of the number of kicks after some value of the kick strength in the quantum case. For $k \geq 5$, the classical phase space is predominantly chaotic and has very small islands that characterize ballistic behaviour. Therefore, the average work trends for $k = 4$ and $k = 5$ were studied. The classical and quantum cases are compared in the figures (5.1) and (5.2).

As seen in the figures, the classical and quantum trends for average and variance of work in the case of $k = 4$ are similar i.e both exhibit diffusive behaviour. But for the case of $k = 5$, we observe dynamical localization setting in for the quantum case while the classical plot shows diffusive behaviour. The above trends are obtained for initial state being ground state i.e temperature $T = 0$. A good question to ask is what will happen to these trends if

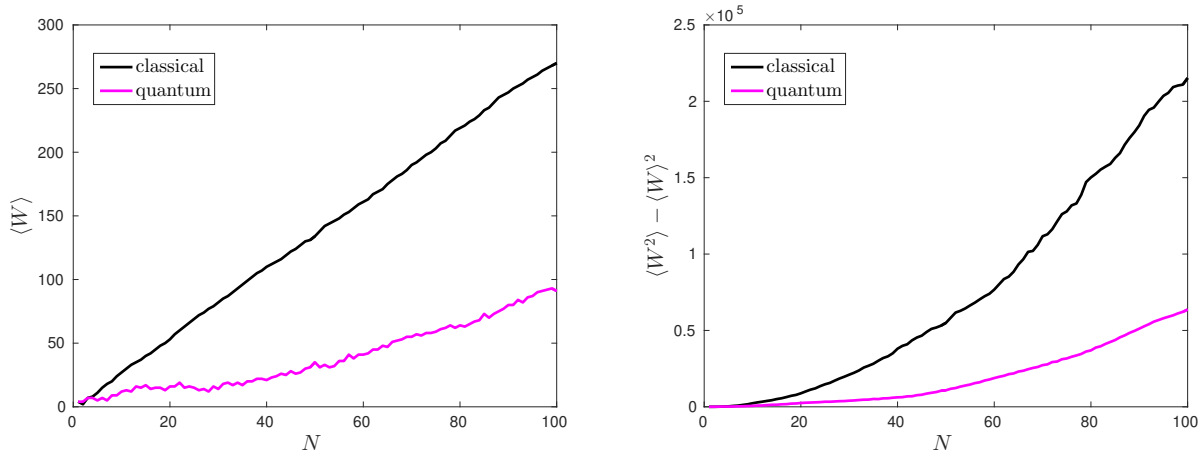

(a) (b)

Figure 5.1: Comparison of classical and quantum trends of (a) Average work and (b) Variance of work for $k = 4$ and $T = 0$

we consider a canonical initial state corresponding to some temperature T. We compared these trends for different temperatures as shown in the following figures (5.3, 5.4, 5.5 and 5.6).

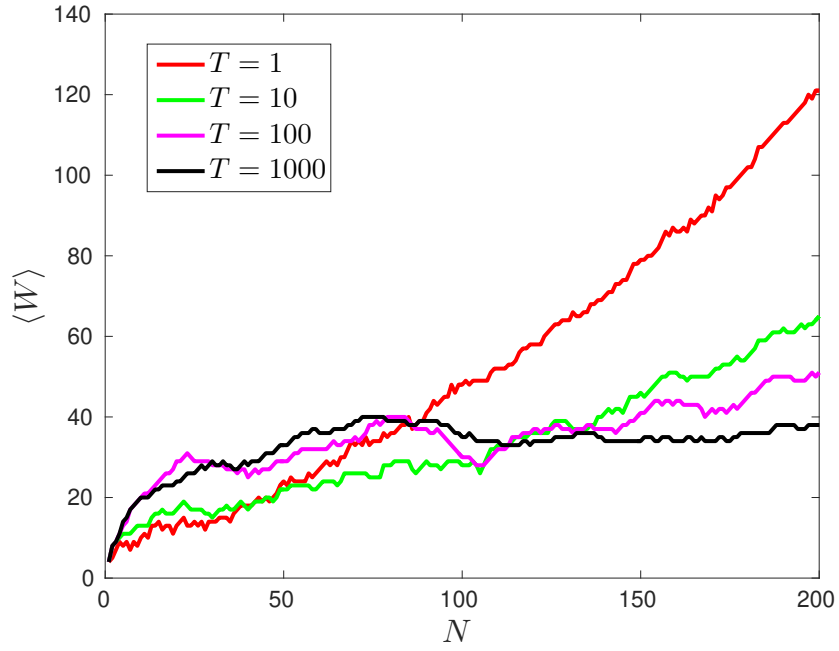

Figure 5.3: Comparison of average quantum work for $k = 4$ and temperatures $T = 1, 10, 100$ and 1000.

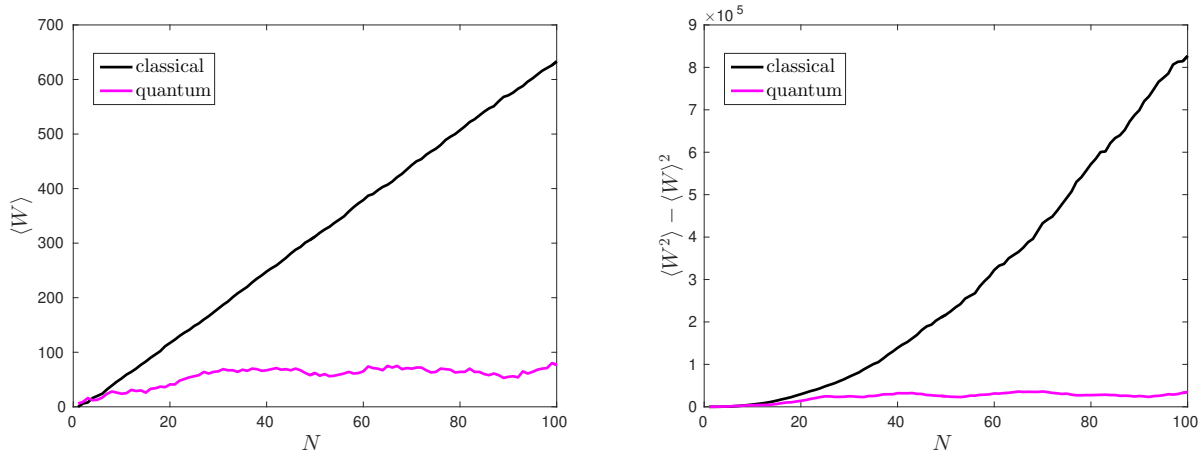

(a) (b)

Figure 5.2: Comparison of classical and quantum trends of (a)Average work and (b) Variance of work for $k = 5$ and $T = 0$

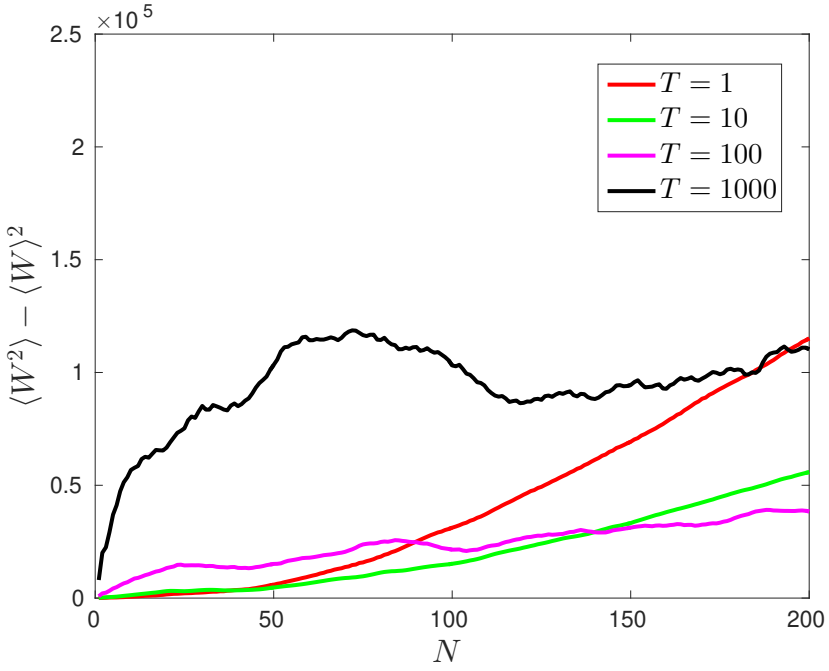

Figure 5.4: Comparison of variance of the quantum work for $k = 4$ and temperatures $T = 1, 10, 100$ and 1000.

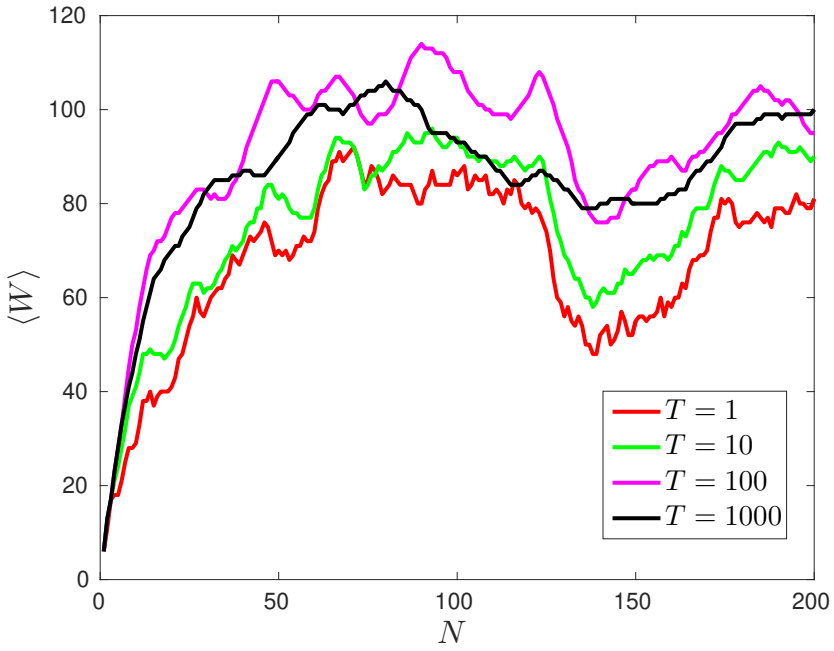

Figure 5.5: Comparison of average quantum work for $k = 5$ and temperatures $T = 1, 10, 100$ and 1000.

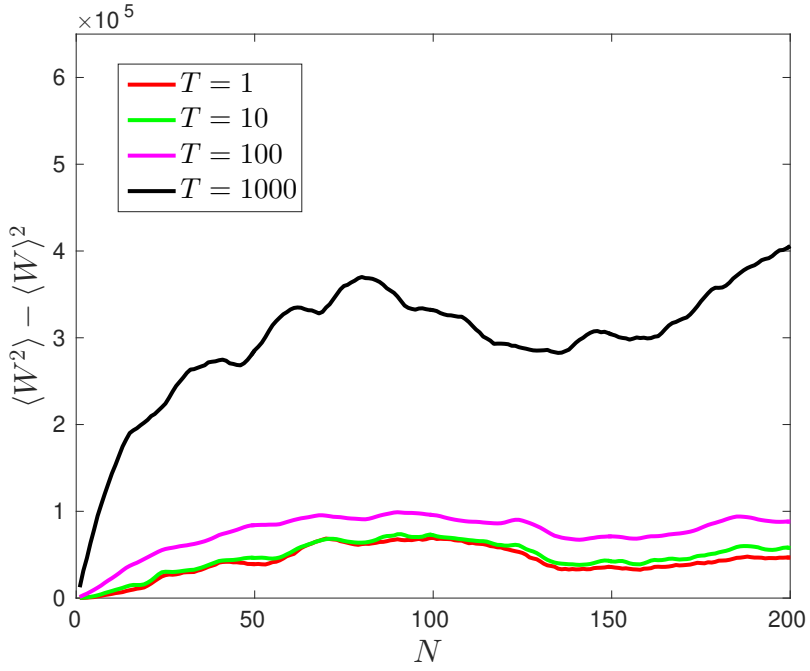

Figure 5.6: Comparison of variance of the quantum work for $k = 5$ and temperatures $T = 1, 10, 100$ and 1000.

We can see that for $k = 5$, the system exhibits dynamical localization even when we increase the temperature. This trend is observed both for the average and the variance of the quantum work. It is interesting to note that for $k = 4$, the behaviour of the system changes from diffusive to exhibiting dynamical localization when the temperature is increased as shown in the figures (5.3) and (5.4). This is yet to be analysed and is a significant part of the future work.

5.2.1 Quantum-Classical correspondence at the level of average and variance of work

As seen in the previous section, the kicked rotor system exhibits very different behaviour in the classical and the quantum regimes. It is therefore interesting to see what happens if we take the $\hbar \to 0$ limit i.e how the trends of average and variance of work change in this limit. This was done again for the cases $k = 4$ and $k = 5$ for temperatures $T = 0$ and $T = 100$. The quantum plots do move closer to classically exhibited one as $\hbar \to 0$ for the all the cases considered as shown in the following figures (5.7), (5.8), (5.9) and (5.10).

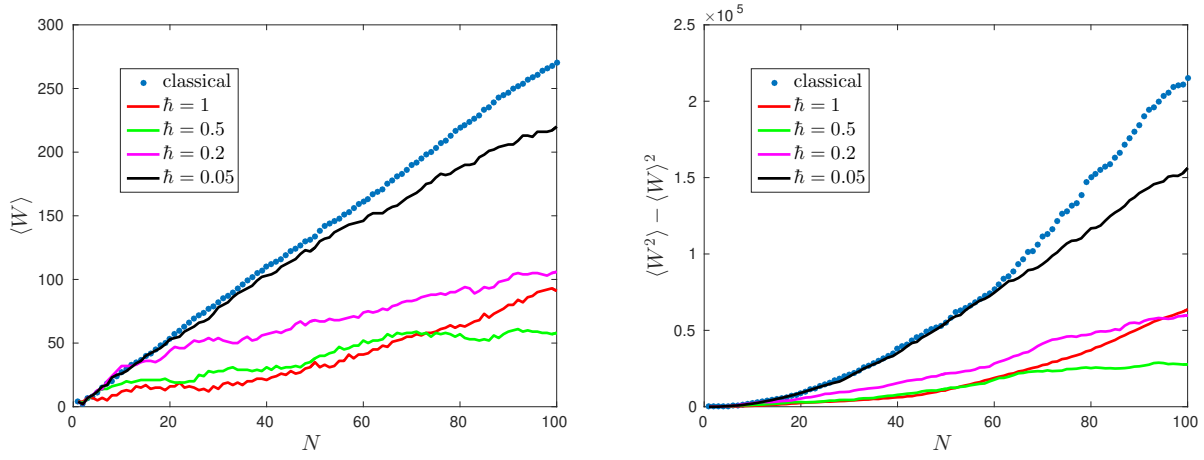

(a) (b)

Figure 5.7: Quantum-Classical correspondence for (a) Average work and (b) Variance of work for $k = 4$ and $T = 0$.

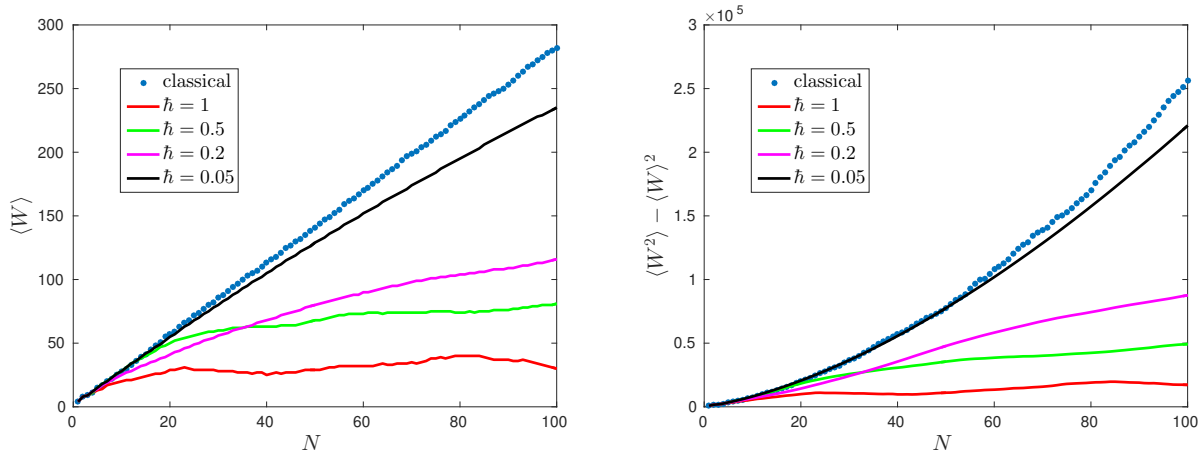

(a) (b)

Figure 5.8: Quantum-Classical correspondence for (a) Average work and (b) Variance of work for $k = 4$ and $T = 100$.

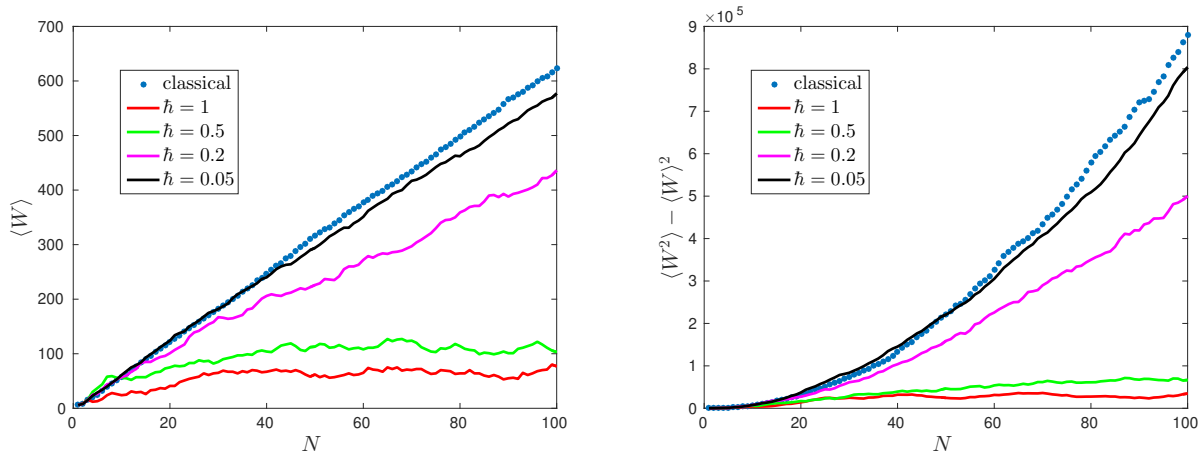

(a) (b)

Figure 5.9: Quantum-Classical correspondence for (a) Average work and (b) Variance of work for $k = 5$ and $T = 0$.

5.3 Work distributions

In this section, I will discuss the work distributions obtained in both the classical and quantum cases.

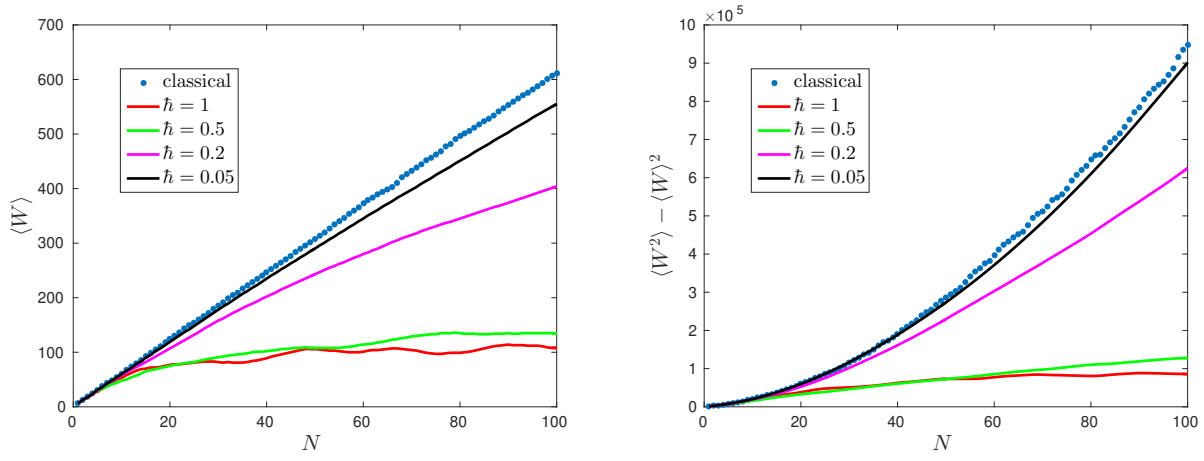

(a) (b)

Figure 5.10: Quantum-Classical correspondence for (a) Average work and (b) Variance of work for $k = 5$ and $T = 100$.

5.3.1 Classical work distributions

We know that the average and variance of work values for the classical kicked rotor system increases linear to N and we therefore expect that the work distributions flatten overtime. The mean value increases with increased number of kicks as shown in the following figures (5.11),(5.12),(5.13). Also,the standard deviation σ increases as $\sqrt{N}$ as indicated by the values. The distributions can be obtained by evolving the initial conditions using the standard map and calculating the work value from the final angular momentum values.

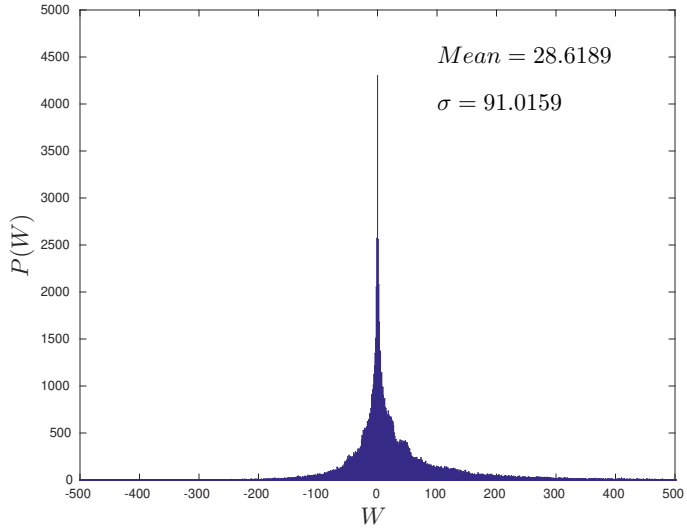

Figure 5.11: Classical work probability density for $k = 4$ and $T = 100$ after $N = 10$.

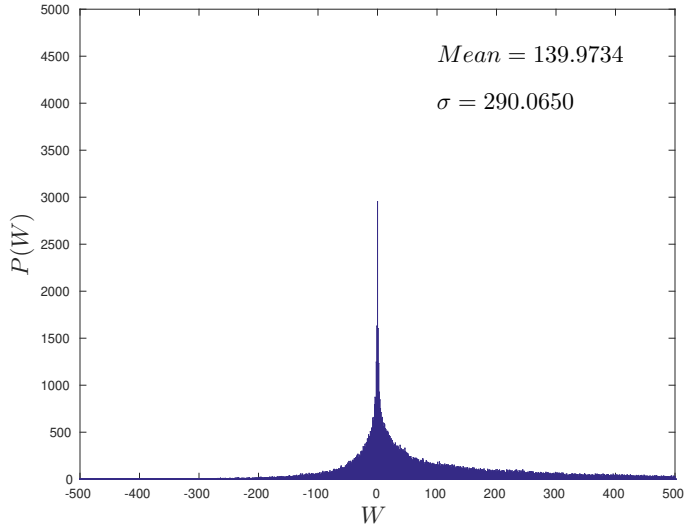

Figure 5.12: Classical work probability density for $k = 4$ and $T = 100$ after $N = 50$.

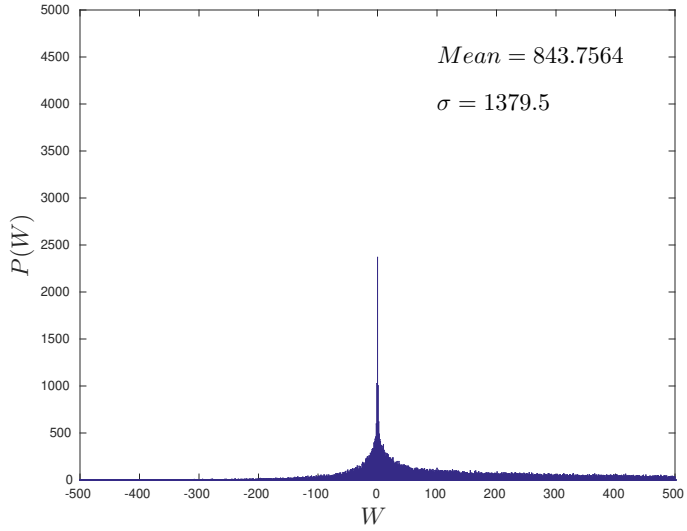

Figure 5.13: Classical work probability density for $k = 4$ and $T = 100$ after $N = 300$.

W/N distributions

As both the average work and variance of work scale linearly with the number of kicks, it is expected that the distribution of W/N should remain saturated i.e the average and the variance of W/N should remain nearly a constant with the number of kicks. This was verified and can be seen in the figures (5.14),(5.15),(5.16).

Verifying crooks relation

Using these classical work distributions, the Crooks relation can be verified. When $\ln\left(\frac{P(W)}{P(-W)}\right)$ is plotted as a function W, we expect to get a linear plot with slope equal to $\beta = 1/T$. This was verified for three different temperatures $T = 1, 2$ and 5 as shown in the following figures (5.17),(5.18). For this we take the bin egde values as the work and the corresponding bin probabilities for obtaining the crooks relation plots.

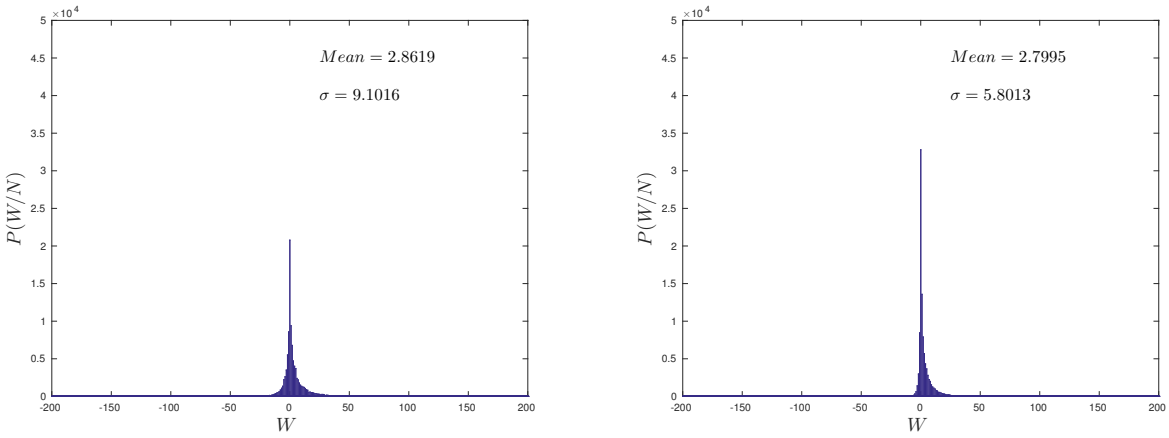

(a) (b)

Figure 5.14: Classical W/N distributions for $k = 4$ at $T = 100$ after (a) $N = 10$ (b) $N = 50$ kicks.

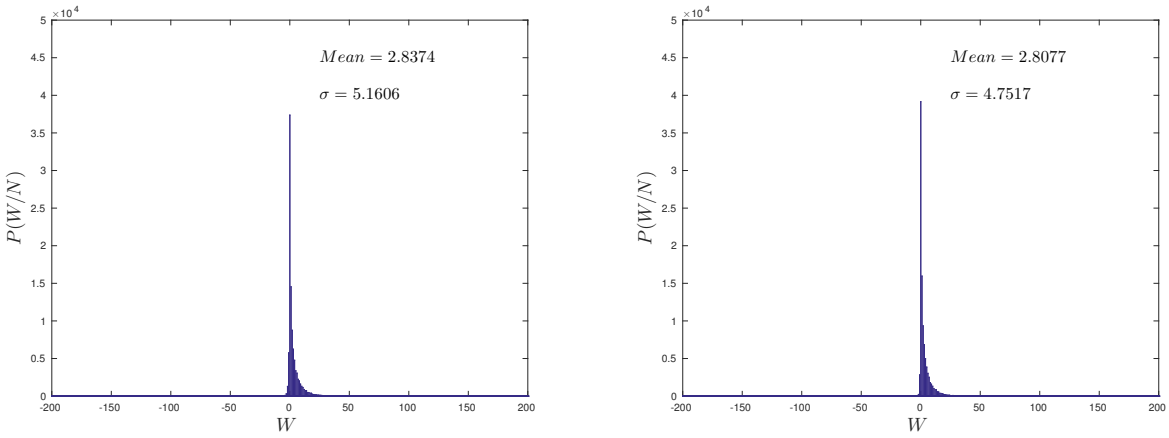

(a) (b)

Figure 5.15: Classical W/N distributions for $k = 4$ at $T = 100$ after (a)$N = 100$ (b) $N = 200$ kicks.

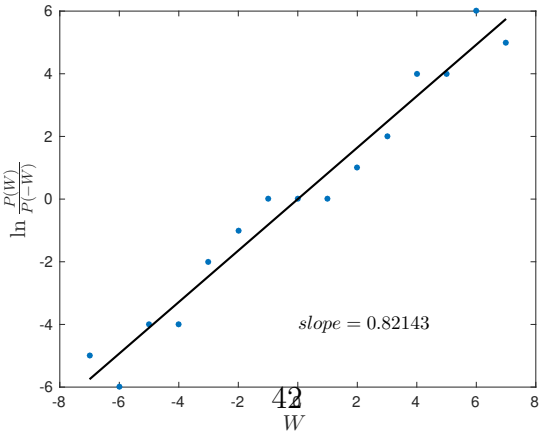

Figure 5.17: Crooks relation for $k = 4$, $N = 1$, $T = 1$

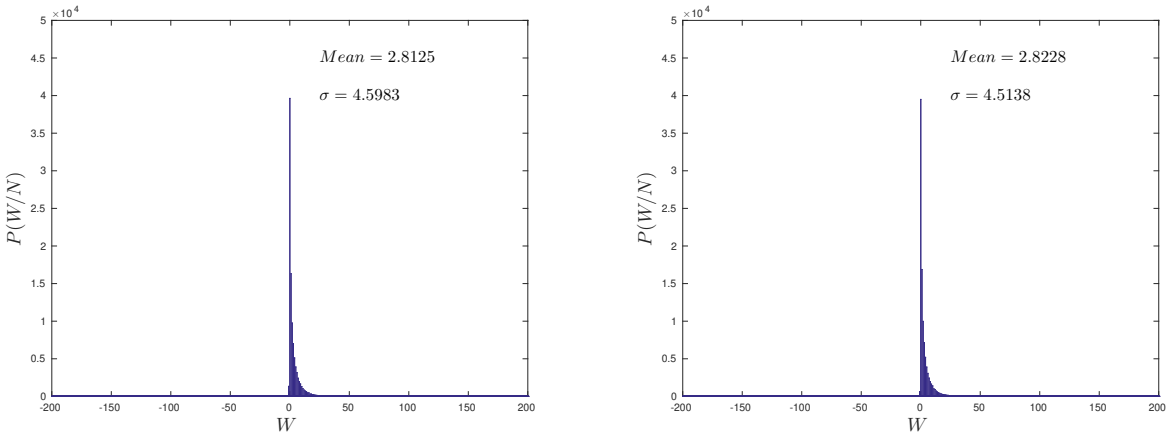

(a) (b)

Figure 5.16: Classical W/N distributions for $k = 4$ at $T = 100$ after (a) $N = 300$ (b) $N = 400$ kicks. It is clear from these plots that the distribution has come to a saturation.

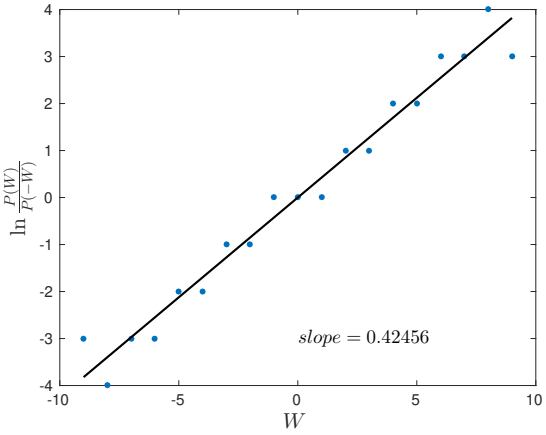

Figure 5.18: Crooks relation for $k = 4$, $N = 1$, $T = 2$

5.3.2 Quantum work distributions

The quantum work distributions have peaks at discrete work values corresponding to difference in the initial and the final energies after multiple transitions due to the kicks. From the plots it is evident that the work probabilities follow the trend suggested by the crooks relation i.e the probability of positive work is more than that of the negative work. This trend is more obvious for lower temperature values. Work distributions were plotted for two

different temperatures $T = 1$ and $T = 100$. The difference is visible from the plots. However, it is very difficult to see dynamical localization at the distribution level unlike in the classical case. The following figures (5.19), (5.20) show the quantum work distributions.

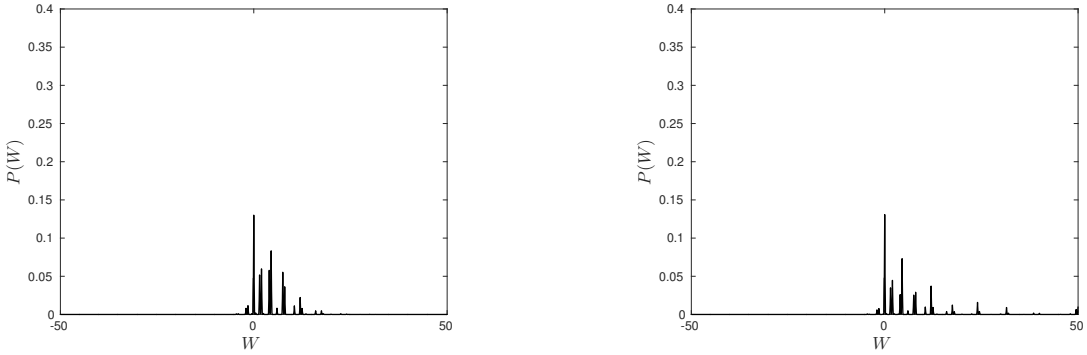

(a) (b) work distribution after 100 kicks

Figure 5.19: quantum work distributions for $k = 4$ at $T = 1$ after (a)$N = 10$ (b) $N = 100$ kicks.

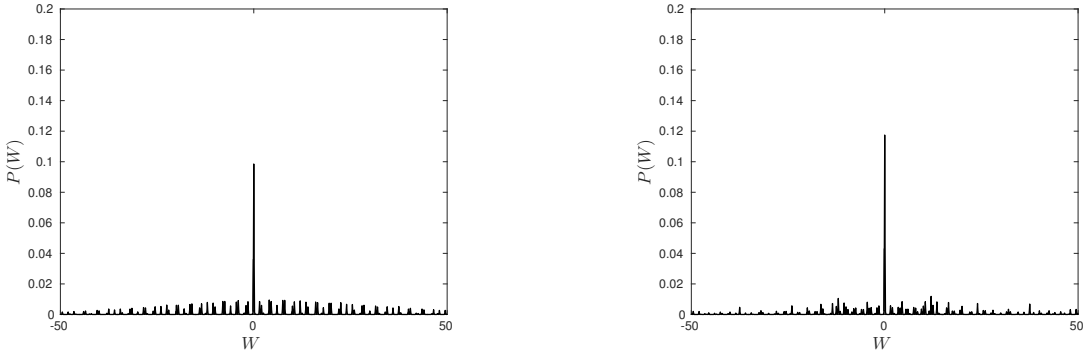

(a) (b)

Figure 5.20: quantum work distributions for $k = 4$ at $T = 100$ after (a) $N = 10$ (b)$N = 100$ kicks.

5.3.3 Quantum-Classical correspondence at the level of work distributions

The quantum-classical correspondence at this level can be seen by taking the limit $\hbar \to 0$ and getting the work distribution for each $\hbar$. These plots does show that the quantum work distribution trends to the classical distribution in the limit. It is important to note that the

quantum work distribution shows a lot of oscillations which increases upon decreasing $\hbar$ and when $\hbar = 0.05$, the oscillations in work distribution cancel out and therefore becomes very similar to the classical distribution. These are shown in the figures (5.21), (5.22).

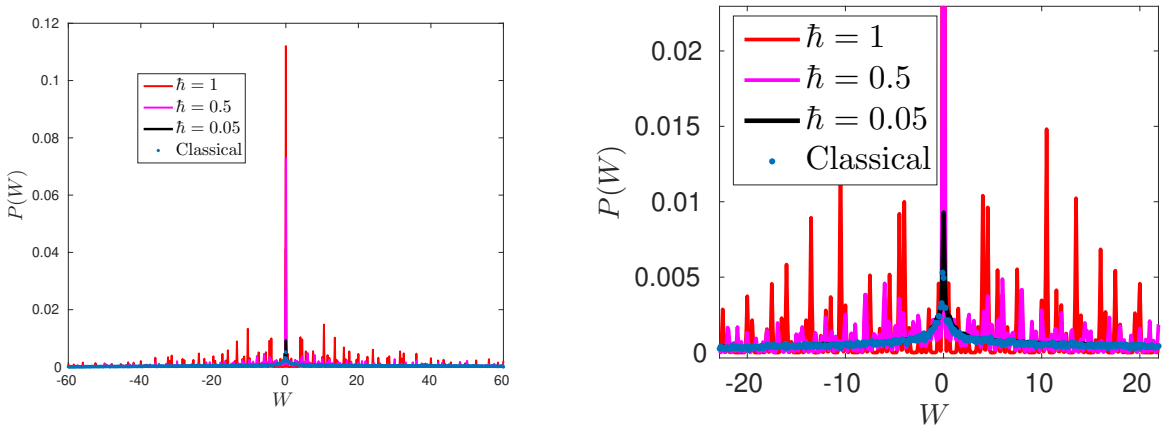

(a) (b)

Figure 5.21: (a) quantum-classical correspondence of work distributions for $k = 4$, $T = 100$ after 60 kicks (b) zoomed version of the same.

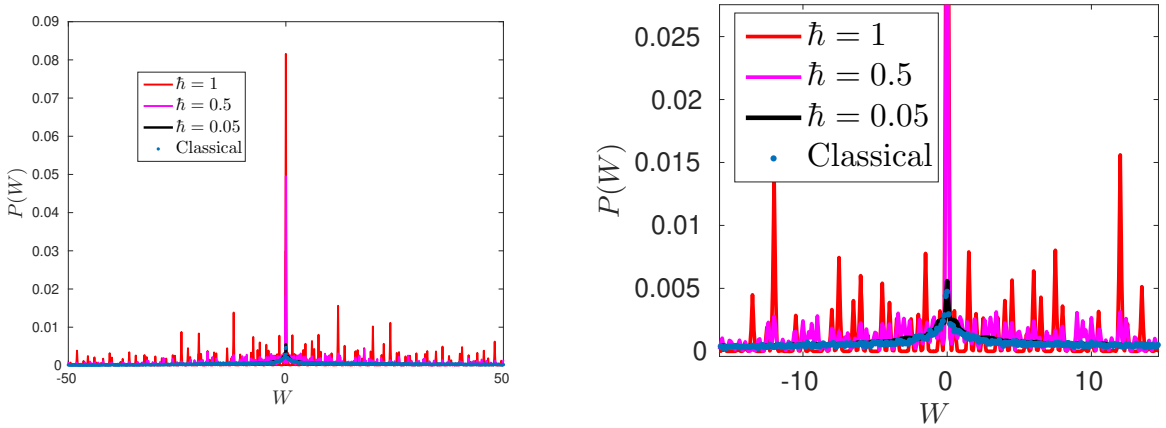

(a) (b)

Figure 5.22: (a) quantum-classical correspondence of work distributions for $k = 4$, $T = 100$ after 90 kicks (b) zoomed version of the same.

5.4 Verification of the thermodynamic uncertainty relation

One of the recent discoveries in the field of stochastic thermodynamics is the thermodynamic uncertainty relation(TUR) which relates the non-equilibrium dissipation and the non-vanishing currents. For systems in non-equilibrium steady state, the TUR gives a relation between the entropy production rate σ and the variance of the non-vanishing current (X) as [16],[18],

$$\sigma \, \frac{Var[X]}{\langle X \rangle^2} \geq 2k_B \tag{5.1}$$

Therefore, the TUR quantifies the trade-off between the precision and the thermodynamic cost. If a similar relation for the dissipated work [17] is considered where the entropy production $\sigma T = W_{dis}$, then we get,

$$\frac{\langle W_{dis}^2 \rangle - \langle W_{dis} \rangle^2}{\langle W_{dis} \rangle} \geq 2k_B T \tag{5.2}$$

We verified this TUR for our system which is an example of a quantum markovian system. It was observed that for different k values and different temperatures, the value of LHS of the equation (5.2) divided by the temperature of the system was greater than 2. This is also captured in the following plots (5.21).

5.5 Conclusion and Future work

In this study on periodically driven kicked rotor system, we investigated the work distributions and their moments as a function of number of kicks given to the system. As expected, we observe diffusive behaviour of moments in the classical case and in the quantum case, we observe dynamical localization. After this we looked at the classical and quantum work distributions and the above mentioned difference in behaviour at the level of distributions.We also verified the Crooks relation using these distributions. On a tangential note, we also examined the trends of the distributions and their moments when the $\hbar \to 0$ limit is taken

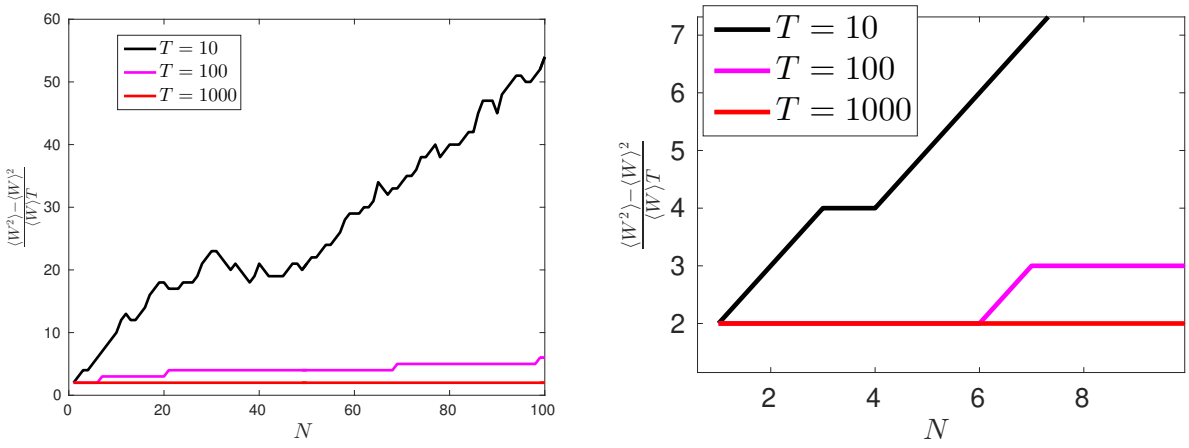

(a) (b)

Figure 5.23: (a)The thermodynamic uncertainty term plotted as a function of number of kicks at different temperatures for $k = 4$. (b) zoomed version of the plot same where it is clear that all three graphs start from above the value 2.

in order to verify the Quantum-Classical correspondence principle. As discussed earlier, we observe a nice transition of the quantum trends to the classical ones as $\hbar \to 0$ limit is taken.

We also investigated the change in trends of average and variance of work when the temperature of the system is increased. The classical diffusive trends for $k = 4$ at $T = 0$, shows localization when temperature is increased while in the case of $k = 5$ where we expect the phase space to be predominantly chaotic, we see localization even when the temperature is increased. It is not yet clear as to why the $k = 4$ case exhibits localization when the temperature is increased. This is an important part for the future work. Other interesting variants of this system that one can study are the double kicked rotor system which consists of two such kicked rotor being kicked with some phase difference and the aperiodically driven kicked rotor system.

Bibliography

[1] Bochkov, G. N., and Yu E. Kuzovlev."General theory of thermal fluctuations in nonlinear systems." Zh. Eksp. Teor. Fiz 72 (1977): 238-243.

[2] Jarzynski, Christopher."Equilibrium free-energy differences from nonequilibrium measurements: A master-equation approach." Physical Review E 56.5 (1997): 5018.

[3] Jarzynski, Christopher. "Nonequilibrium equality for free energy differences." Physical Review Letters 78.14 (1997): 2690.

[4] Jarzynski, Christopher."Equalities and inequalities: Irreversibility and the second law of thermodynamics at the nanoscale." Annu. Rev. Condens. Matter Phys. 2.1 (2011): 329-351.

[5] Crooks, G. E., 1999,"Entropy production fluctuation theorem and the nonequilibrium work relation for free energy differences" Phys. Rev. E 60, 2721.

[6] Campisi, Michele, Peter Hnggi, and Peter Talkner. "Colloquium: Quantum fluctuation relations: Foundations and applications." Reviews of Modern Physics 83.3 (2011): 771.

[7] Esposito, Massimiliano, Upendra Harbola, and Shaul Mukamel."Nonequilibrium fluctuations, fluctuation theorems, and counting statistics in quantum systems." Reviews of modern physics 81.4 (2009): 1665.

[8] Campisi, Michele, Peter Talkner, and Peter Hnggi."Fluctuation theorem for arbitrary open quantum systems." Physical review letters 102.21 (2009): 210401.

[9] Jarzynski, Chris."Nonequilibrium work theorem for a system strongly coupled to a thermal environment." Journal of Statistical Mechanics: Theory and Experiment 2004.09 (2004): P09005.

[10] Stckmann, Hans-Jrgen. "Quantum chaos: an introduction." (2000): 777-778.

[11] Lichtenberg, Allan J., and Michael A. Lieberman. Regular and stochastic motion. Vol. 38. Springer Science and Business Media, 2013.

[12] Casati, Giulio, et al. "Stochastic behavior of a quantum pendulum under a periodic perturbation." Stochastic behavior in classical and quantum Hamiltonian systems. Springer, Berlin, Heidelberg, 1979. 334-352.

[13] Chirikov, Boris, and Dima Shepelyansky. "Chirikov standard map." Scholarpedia 3.3 (2008): 3550.

[14] Delande, Dominique. "Kicked rotor and Anderson localization." Boulder School on Condensed Matter Physics (2013).

[15] Grempel, D. R. "DR Grempel, RE Prange, and S. Fishman, Phys. Rev. A 29, 1639 (1984)." Phys. Rev. A 29 (1984): 1639.

[16] Barato, Andre C., and Udo Seifert. "Thermodynamic uncertainty relation for biomolecular processes." Physical review letters 114.15 (2015): 158101.

[17] Manikandan, Sreekanth K., and Supriya Krishnamurthy. "Exact results for the finite time thermodynamic uncertainty relation." Journal of Physics A: Mathematical and Theoretical 51.11 (2018): 11LT01.

[18] Horowitz, Jordan M., and Todd R. Gingrich. "Proof of the finite-time thermodynamic uncertainty relation for steady-state currents." Physical Review E 96.2 (2017): 020103.